Appl. Phys. B 80, 871–874 (2005)
DOI: 10.1007/s00340-005-1790-9

Applied Physics B
Lasers and Optics

H.Y. XU[1,2]
Y.C. LIU[2,✉]
Y.X. LIU[2]
C.S. XU[2]
C.L. SHAO[2]
R. MU[3]

Ultraviolet electroluminescence from p-GaN/i-ZnO/n-ZnO heterojunction light-emitting diodes

[1]Key Laboratory of Excited State Processes, Changchun Institute of Optics, Fine Mechanics and Physics, Chinese Academy of Sciences, Changchun, PRC
[2]Center for Advanced Opto-electronic Functional Material Research, Northeast Normal University, Changchun, PRC
[3]Nanoscale Materials and Sensors Lab, Department of Physics, Fisk University, Nashville, TN

Received: 26 January 2005
Published online: 22 April 2005 • **© Springer-Verlag 2005**

ABSTRACT In this work, we report on the fabrication and characteristics of light-emitting diodes based on p-GaN/i-ZnO/n-ZnO heterojunction. A 30 nm i-ZnO layer was grown on p-GaN by rf reactive magnetron sputtering, then a n-ZnO was deposited by the electron beam evaporation technique. The current-voltage characteristic of the obtained p-i-n heterojunction exhibited a diode-like rectifying behavior. Because the electrons from n-ZnO and the holes from p-GaN could be injected into a i-ZnO layer with a relatively low carrier concentration and mobility, the radiative recombination was mainly confined in i-ZnO region. As a result, an ultraviolet electro-emission at 3.21 eV, related to ZnO exciton recombination, was observed in a room-temperature electroluminescence spectrum of p-i-n heterojunction under forward bias.

PACS 78.60.Fi; 73.40.Lq; 85.60.Jb

1 Introduction

ZnO, a wide bandgap (3.37 eV) semiconductor with a large exciton binding energy (60 meV), is a promising material for optoelectronic applications [1–6]. Recently, Tsukazaki et al. [4] reported the significant advance in light-emitting diodes (LEDs) based on ZnO homojunction, which has led ZnO to gain much more attention for applications in short-wavelength LEDs and laser diodes suitable for high-temperature operation. However, until now, the lack of reliable, high-quality, p-type ZnO has hampered the development of ZnO homostructural ultraviolet (UV) LEDs, though much progress has been made in this area [7–9]. Thereby, constructing heterojunction LEDs with ZnO active regions becomes another attractive choice.

ZnO and GaN are similar in many of their physical properties. For example, ZnO and GaN both have a wurtzite crystal structure, almost the same in-plane lattice parameter (the lattice mismatch ∼1.8%), and room-temperature bandgaps of 3.37 and 3.4 eV, respectively. Currently, the high-quality p-type GaN (p-GaN) has been successfully obtained, even commercially supplied. Based on their similar material properties and the relative availability of p-GaN, recently, several groups have fabricated the heterojunction LEDs by combining p-GaN with n-type ZnO (n-ZnO) [10, 11]. These GaN/ZnO LEDs exhibit the improved carriers confinement compared to homojunction, which leads to higher recombination and improved device efficiency. However, due to relatively lower carrier concentration and mobility of p-GaN compared with those of n-ZnO, the blue-violet electroluminescence (EL) of those reported GaN/ZnO heterojunctions usually originates from GaN layer, while UV EL related to ZnO exciton recombination is not observed.

In this work, a thin semi-insulating ZnO (i-ZnO) layer with high resistivity of ∼1.3 kΩ cm was inserted between the p-GaN and n-ZnO layer, to form p-i-n heterojunction, which confined parts of carriers to recombine in i-ZnO region. As a result, 3.21 eV (386 nm) EL from this p-i-n heterojunction, related to ZnO exciton recombination, was observed at room-temperature (RT).

2 Experiments

Figure 1 shows a schematic diagram of p-GaN/i-ZnO/n-ZnO heterojunction LEDs. Mg doped p-GaN epitaxial film, which was grown on Al_2O_3 (0001) by metal organic chemical vapor deposition, was commercially purchased and served as substrate. A thin i-ZnO layer with the thickness of ∼30 nm was deposited on p-GaN by rf reactive magnetron sputtering. An ultrapure metallic zinc disk was used as the sputtering target. Ultrapure Ar and O_2 gas mixtures with the flow-rate ratio of 2:1 were introduced into the growth chamber. The substrate temperature and rf power density were controlled at 300 °C and 2.0 W/cm^2 during film deposition, respectively. The working pressure was kept at 1.0 Pa. Next, an n-ZnO layer was grown by electron beam evaporating ZnO ceramic target. Higher evaporation power density (195 W/cm^2)

✉ E-mail: ycliu@nenu.edu.cn

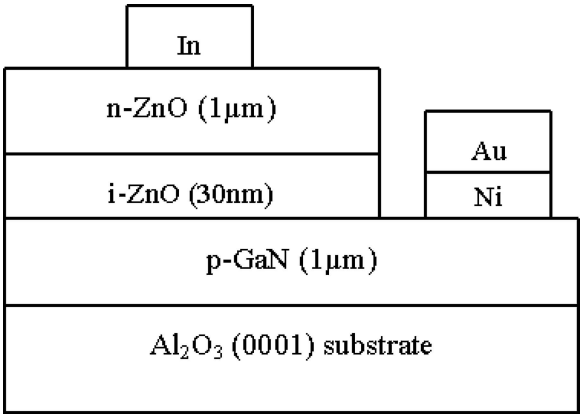

FIGURE 1 Schematic diagram of p-GaN/i-ZnO/n-ZnO heterojunction LEDs

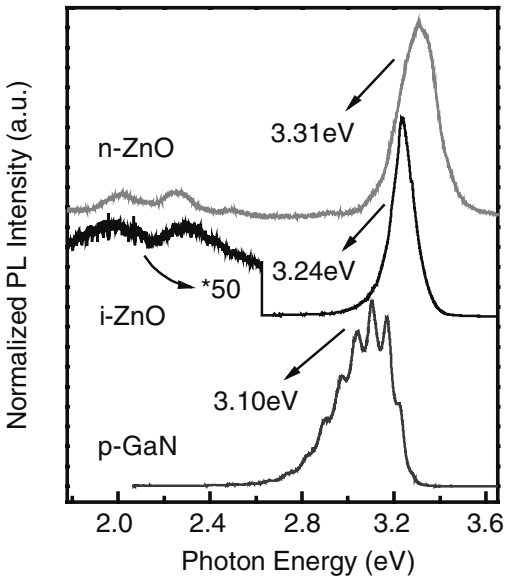

FIGURE 2 RT PL spectra of p-GaN, i-ZnO and n-ZnO

and substrate temperature (500 °C) were used for obtaining n-ZnO with higher electron concentration. Moreover, for comparison, GaN/ZnO p-n heterojunction was also fabricated under the same conditions. Ohmic contact to p-GaN was made by thermally evaporating Ni/Au. Indium electrode was soldered on n-ZnO layer at 300 °C in vacuum. Electrical parameters of individual layers and current-voltage (I–V) characteristic of heterojunction were measured by using the Hall system (Model 7707, LakeShore Co.). Good ohmic contact was verified before measurement. RT EL spectra were collected from the edge of top electrode under forward bias by using fluorescence spectrometer (LS-55, Perkin Elmer Co.). Photoluminescence (PL) measurements were conducted with micro-Raman spectrometer (Jobin Yvon Co.). The 325 nm line of a He-Cd laser was used as the excitation source.

3 Results and discussion

The electrical parameters of p-GaN, i- and n-ZnO were listed in Table 1. The nonstochiometric undoped ZnO films usually exhibit n-type conductivity due to the 'native donor' (oxygen vacancies and zinc interstitials). Hence, the low-resistive films can be obtained by controlling these native defects. During n-ZnO deposition, high-energy electrons beam can break some of the Zn-O bonds, and the dissociative Zn^{2+} ions are easier to combine with the substrate than O^{2-} ions do. These resulted in the formation of Zn-rich film, thus, the higher electron concentration ($7.53 \times 10^{18}\,cm^{-3}$) of n-ZnO was attributed to the generation of oxygen vacancies and zinc interstitials. However, i-ZnO was grown in an oxygen-rich environment, which effectively decreased the 'native donor', thus, resulting in low carrier concentration. As for the low carrier mobility in i-ZnO layer, it may be attributed to the grain-boundary and interface scattering [12].

Samples	ρ (Ω cm)	μ ($cm^2\,V^{-1}\,s^{-1}$)	N (cm^{-3})
p-GaN	1.63	5.34	7.13×10^{17}
i-ZnO	1.12×10^{3}	1.28	4.38×10^{15}
n-ZnO	4.14×10^{-2}	20.0	7.53×10^{18}

TABLE 1 The resistivity ρ, carrier concentration N and mobility μ of p-GaN, i-ZnO and n-ZnO

The RT PL spectra of individual layers were showed in Fig. 2. The PL spectrum of p-GaN showed only a strong emission centered at 3.10 eV with multi-reflection interference fringes. This band was generally attributed to transitions from the conduction band or unidentified shallow donors to deep Mg acceptors levels [10, 11]. The UV near-band-edge (NBE) emission from GaN was not observed. Both i- and n-ZnO displayed three emission bands: an UV NBE emission which originates from the recombination of ZnO free and bound excitons, a deep-level green emission at ∼2.3 eV, and orange emission at ∼1.95 eV. It is generally accepted that the green and orange emission are associated with oxygen vacancies and zinc interstitials in ZnO crystal lattice [13–16]. The UV emissions of i- and n-ZnO were located at 3.24 and 3.31 eV, respectively. The relative shift (70 meV) of UV emission may be attributed to the Burstein–Moss effect [17]. That is, the electronic states near the bottom of the conduction band are filled because of the high carrier concentration, which induces the widened optical bandgap. Moreover, the deep-level emission of n-ZnO was far stronger than that of i-ZnO, which indicated the relatively higher concentration of native donor defects in n-ZnO. This PL result was well consistent with aforementioned electrical properties of ZnO layers.

The RT I–V characteristics of the GaN/ZnO p-n and p-i-n heterojunctions were shown in Fig. 3. Both exhibited a rectifying, diode-like behavior. For p-GaN/n-ZnO heterojunction, the forward turn-on and reverse breakdown voltages was ∼3 and ∼4 V, respectively. The relatively low forward and reverse threshold voltages are probably due to the existence of interface defects [10, 18], especially extended defects in n-ZnO. In contrast with I–V characteristics of p-n heterojunctions, due to the insertion of high-resistive i-ZnO layer, the relatively higher turn-on voltage for forward (∼10 V) and reverse (∼11 V) bias were obtained in p-i-n heterojunction, although the turn on appeared very soft.

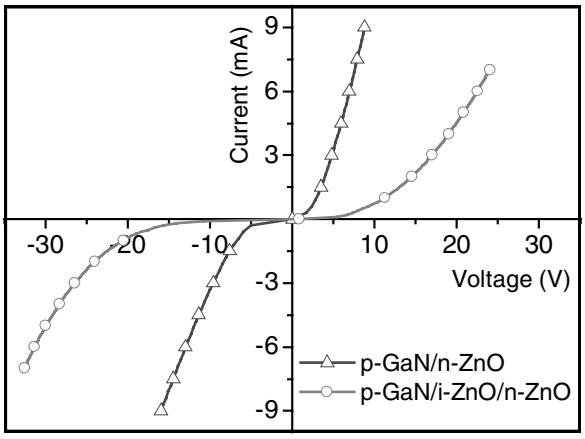

FIGURE 3 RT I–V characteristics of the GaN/ZnO p-n and p-i-n heterojunctions

Figure 4 showed the RT EL spectra of the GaN/ZnO p-n and p-i-n heterojunctions LEDs. A broad emission band centered at 3.08 eV (403 nm) with a tail extended to longer wavelength was observed in the EL spectrum of p-n heterojunction LED under forward bias. A comparison between EL and PL spectra showed that the lineshape and peak position of EL from p-n heterojunction was very similar to that of PL from p-GaN (3.1 eV). Thereby, the 3.08 eV EL was reasonably attributed to Mg-levels related emission in p-GaN layer. Similar EL results had been reported in ref. 10 and 11. In order to understand the reason why EL of p-n heterojunction originated from the p-GaN side, we first considered their energy band structure. The electron affinities of ZnO (χ_{ZnO}) and GaN (χ_{GaN}) are 4.35 and 4.2 eV [19], while the bandgaps of ZnO (Eg_{ZnO}) and GaN (Eg_{GaN}) are 3.37 and 3.4 eV, respectively. Based on the Anderson model [20], the conduction band offset is $\Delta Ec = \chi_{ZnO} - \chi_{GaN} = 0.15$ eV, and the valence band offset is $\Delta Ev = Eg_{ZnO} + \Delta Ec - Eg_{GaN} = 0.12$ eV. The aforementioned calculations showed that the electrons in n-ZnO and holes in p-GaN overcame almost equal barriers to realize the carrier injection, that is, the type-II band alignment at the ZnO/GaN heterointerface has a much weaker effect on EL of p-n heterojunction. Thereby, the origin of EL would be mainly determined by the differences of carrier mobility and concentration between n-ZnO and p-GaN. As shown in Table 1, the carrier concentration and mobility in n-ZnO was much larger than that of the hole in p-GaN. Thereby, the electrons injection from n-ZnO to p-GaN could overcome the holes injection from p-GaN to n-ZnO. The radiative recombination mainly occurred in the p-GaN side of p-GaN/n-ZnO heterojunction.

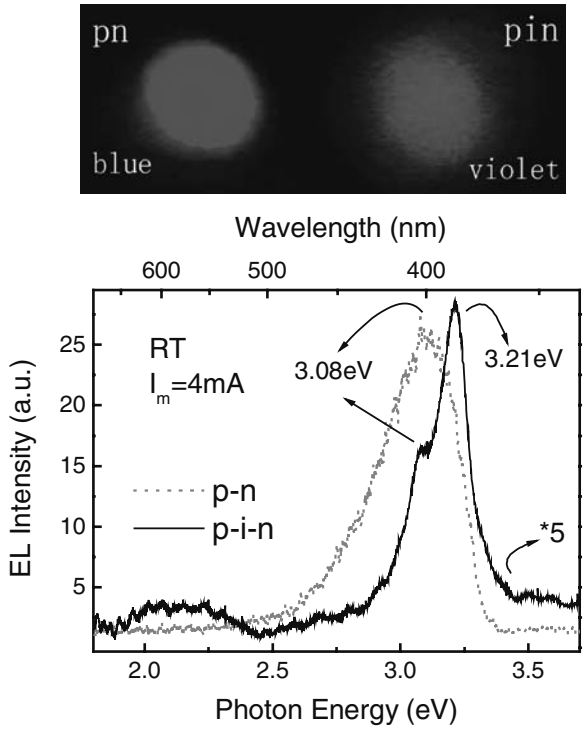

FIGURE 4 Magnified photographs of light output and RT EL spectra of the GaN/ZnO p-n and p-i-n heterojunctions LEDs (Injection current, $I_m = 4$ mA)

In order to obtain EL from ZnO, a thin i-ZnO layer was inserted, to form p-i-n heterojunction, as shown in Fig. 1. Because i-ZnO has the lowest carrier concentration and mobility among the three layers, we can expect that the carriers including holes from p-GaN and electrons from n-ZnO can inject into i-ZnO layer, where the radiative recombination occurs. As expected, different from the EL of p-n heterojunction, two new emissions, including a narrow UV EL peak at 3.21 eV and a very broad, weak emission band at ~2.1 eV, were observed in the EL spectrum of p-i-n heterojunction, as shown in Fig. 4. Both emissions were located at almost the same positions as those in PL spectra of i-ZnO. Thus, 3.21 and ~2.1 eV EL bands were believed to originate from the active i-ZnO region, and were attributed to UV NBE emission related to ZnO exciton recombination and deep-level emission related to native defects, respectively. Moreover, a relatively weak emission at 3.08 eV, which had been proved to be from p-GaN layer, was also detected in EL spectrum of p-i-n heterojunction. The possible reason was that a small quantity of electrons tunneled though i-ZnO layer, and were injected into p-GaN region. The observation of ZnO EL confirmed that the radiative recombination can be partly confined in i-ZnO region by constructing p-i-n heterojunction. By further optimizing the device structure, it is possible to suppress, even eliminate the EL band from p-GaN.

4 Conclusion

In conclusion, we fabricated p-GaN/i-ZnO/n-ZnO heterojunction LEDs. The I–V curve showed a diode characteristic. By constructing p-i-n heterojunction, the radiative recombination was partly transferred from p-GaN to i-ZnO region. Thereby, an UV EL at 3.21 eV, related to ZnO exciton recombination, was obtained from p-i-n heterojunction. Due to high exciton binding energy (60 meV) of ZnO, such p-i-n heterojunction has the potential applications in UV LEDs and laser diode durable at high-temperature operation.

ACKNOWLEDGEMENTS This work is supported by Cultivation Fund of the Key Scientific and Technical Innovation Project (No. 704017), Ministry of Education of China; National Natural Science Foundation of China (No. 60376009, 60278031).

REFERENCES

1 H. Cao, J.Y. Xu, E.W. Seeling, R.P.H. Chang, Appl. Phys. Lett. **76**, 2997 (2000); Phys. Rev. Lett. **84**, 5584 (2000).
2 Z.K. Tang, G.K.L. Wong, P. Yu, M. Kawasaki, A. Ohtomo, H. Koinuma, Y. Segawa, Appl. Phys. Lett. **72**, 3270 (1998)
3 T. Aoki, Y. Hatanaka, D.C. Look, Appl. Phys. Lett. **76**, 3257 (2000)
4 A. Tsukazaki, A. Ohtomo, T. Onuma, et al., Nat. Mater. **4**, 47 (2005)
5 P.F. Carcia, R.S. McLean, M.H. Reilly, G.N. Jr, Appl. Phys. Lett. **82**, 1117 (2003)
6 C.P. Park, I.S. Jeong, J.H. Kim, S. Im, Appl. Phys. Lett. **82**, 3973 (2003)
7 D.C. Look, D.C. Reynolds, C.W. Litton, R.L. Jones, D.B. Eason, G. Cantwel, Appl. Phys. Lett. **81**, 1830 (2002)
8 K.K. Kim, H.S. Kim, D.K. Hwang, J.H. Lim, S.J. Park, Appl. Phys. Lett. **83**, 63 (2003)
9 Y.R. Ryu, T.S. Lee, J.H. Leem, H.W. White, Appl. Phys. Lett. **83**, 4032 (2003)
10 Ya.I. Alivov, J.E. Van Nostrand, D.C. Look, M.V. Chukichev, B.M. Ataev, Appl. Phys. Lett. **83**, 2943 (2003)
11 Q.X. Yu, B. Xu, Q.H. Wu, Y. Liao, G.Z. Wang, R.C. Fang, H.Y. Lee, C.T. Lee, Appl. Phys. Lett. **83**, 4713 (2003)
12 Z.L. Pei, C. Sun, M.H. Tan, J.Q. Xiao, D.H. Guan, R.F. Huang, L.S. Wen, J. Appl. Phys. **90**, 3432 (2001)
13 A.V. Dijken, E.A. Meulenkamp, D. Vanmaekelbergh, A. Meijerink, J. Phys. Chem. B. **104**, 715 (2000)
14 K. Vanheusden, C.H. Seager, W.L. Warren, D.R. Tallant, J.A. Voigt, Appl. Phys. Lett. **68**, 403 (1996)
15 H.Y. Xu, Y.C. Liu, J.G. Ma, Y.M. Luo, Y.M. Lu, D.Z. Shen, J.Y. Zhang, X.W. Fan, R. Mu, J. Phys.: Condens. Matter **16**, 5143 (2004)
16 L. Spanhel, M.A. Anderson, J. Am. Chem. Soc. **113**, 2826 (1991)
17 E. Burstein, Phys. Rev. **93**, 632 (1954)
18 D.K. Zhang, Y.C. Liu, Y.L. Liu, H. Yang, Physica B **351**, 178 (2004)
19 Ya.I. Alivov, E.V. Kalinina A.E. Cherenkov, D.C. Look, B.M. Ataev, A.K. Omaev, M.V. Chukichev, D.M. Bagnall, Appl. Phys. Lett. **83**, 4719 (2003)
20 A.G. Milnes, D.L.Feucht, *Heterojunctions and Metal-Semiconductor Junctions* (Academic, New York, 1972)